

Towed sensors positioning with forward looking sonars: Application on a Side Scan Sonar

Isabelle Leblond, Alain Bertholom

▶ **To cite this version:**

Isabelle Leblond, Alain Bertholom. Towed sensors positioning with forward looking sonars: Application on a Side Scan Sonar. e-Forum Acusticum 2020, Dec 2020, Lyon, France. pp.1981-1988, 10.48465/fa.2020.0315 . hal-03240240

HAL Id: hal-03240240
https://hal.science/hal-03240240

Submitted on 28 May 2021

HAL is a multi-disciplinary open access archive for the deposit and dissemination of scientific research documents, whether they are published or not. The documents may come from teaching and research institutions in France or abroad, or from public or private research centers.

L'archive ouverte pluridisciplinaire **HAL**, est destinée au dépôt et à la diffusion de documents scientifiques de niveau recherche, publiés ou non, émanant des établissements d'enseignement et de recherche français ou étrangers, des laboratoires publics ou privés.

TOWED SENSORS POSITIONING WITH FORWARD LOOKING SONARS. APPLICATION ON A SIDE SCAN SONAR

Isabelle Leblond[1] **Alain Bertholom**[2]
[1]Irenav EA3634, Ecole Navale
BCRM Brest, Ecole Navale, CC600 29240 BREST CEDEX 9
[2] Lab-STICC UMR CNRS 6285, ENSTA Bretagne
2 rue François Verny 29806 BREST CEDEX 9
isabelle.leblond@ecole-navale.fr

ABSTRACT

In order to have good data quality, sensors like sidescan sonars (SSS) or magnetometers have to be deployed near the seabed. So, they are often carried by a towfish and linked via an umbilical cable to the ship. Unfortunately, because the cable is frequently not tensioned or not in the axis of the vessel, their ship relative position is difficult to estimate. A first solution to solve this problem is to use an ultra-short baseline (USBL) to obtain a positioning of the sensor with respect to the vessel, but this device is not always available or suitable. The solution proposed here is to use a forward looking sonar (FLS) to track the positioning of the towfish. A first part of this work is dedicated to show the experimental conditions. A second section is devoted to the tracking of the fish reflector in the FLS image, performed by an image processing module. This work is applied here on SSS data, so, the third part of this article is expended to carry out the image sonar mosaicing in a geographical information system (GIS). The different SSS mosaics results are compared to the digital terrain models (DTM) of the same area, showing an error positioning of about one meter.

1. INTRODUCTION

In oceanographic surveys, it is sometimes necessary to put the used device on a towfish. It is the case of Sidescan Sonars (SSS) for example, which gives images of the seabed reflectivity. Nature of seafloor and objects are the represented by acoustic echoes and shadows. Images quality is given by elongated shadows, which is obtained when the sonar is near the seabed (~10 m above it) [1]. It is also the case of magnetometers [2], which record magnetic anomalies on the seabed. Because of the magnetic signal decrease in R^3 (R the distance to the target), this sensor must be near the seabed and far the ship. Remotely Operated Vehicles (ROV), by their nature, are also deployed near the seafloor.

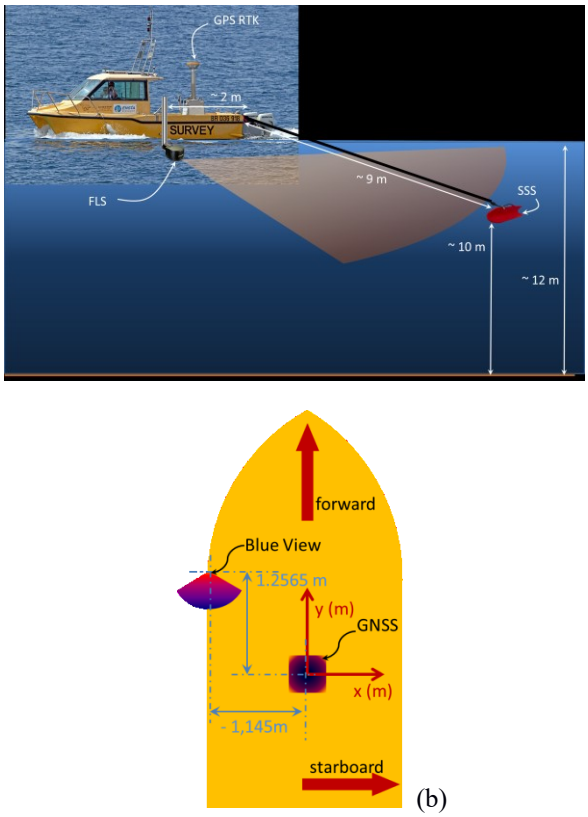
For different reasons, data recorded by these sensors should be georeferenced, for example to obtain magnetic anomalies maps, SSS images mosaics or precisely located photogrammetry. Unfortunately, there is imprecisions in towfish localization, because of the absence of GNSS in the underwater case, but also because of navigation variations of the towfish behind the ship (drift, depth variations, etc.) [3]. Several solutions are usually employed to reduce the imprecision of the towfish localization: the first solution is to add a layback to the towfish position, which is, in a first approximation, simply a trigonometric relationship between the cable length and the towfish altitude [4]. To take into account the real shape of the cable, which is often not straight, a layback model may replace it [5]. But in all cases, the towfish is supposed to be behind the ship, which is not always the case in reality. To find the real towfish positions, acoustic ranging systems like Long Baseline (LBL) or Ultra-short Baseline (USBL) should be used [4]. Unfortunately, these devices should sometimes be not suitable: it is the case of magnetometers for example, where acoustic transponders should generate magnetic perturbations. In the same way, these devices are sometimes not available, and another solutions should be found.

The work proposed here intends to verify the feasibility of using a Forward Looking Sonar (FLS) to track towfish positions during the time. The first chapter is devoted to a description of the experiment. A second chapter describes the tracking algorithm in FLS images. A third chapter explains the projection of SSS images in a geographical map and the last chapter estimates objects errors positioning by a comparison with a bathymetric map. In the end, perspectives to this work will conclude the statements.

2. DESCRIPTION OF THE EXPERIMENT

The experiment was realized in Brest Harbor with a SSS Starfish 450, trailed by a little hydrographic launch. To follow the trajectory of the SSS during the survey, a FLS Blueview P900-130 was mounted on a pole which is located at port side and insonifying back. There is also a RTK GNSS, mounted on another pole, quite in the middle of the ship. **Figure** 1 shows drawings of the experimental protocol. **Table** 1 and **Table** 2 give the principal characteristics of the two sonars.

The survey was consisting in several parallel lines of approximately 500 meters long, insonified successively and oriented quite north-south. For each line, SSS and FLS data are recorded simultaneously. A particular attention must be made to the time synchronization between the different devices (use of the UTC time recommended). **Figure** 2 shows the area of the experiment and the realized trajectory.



(a) (b)

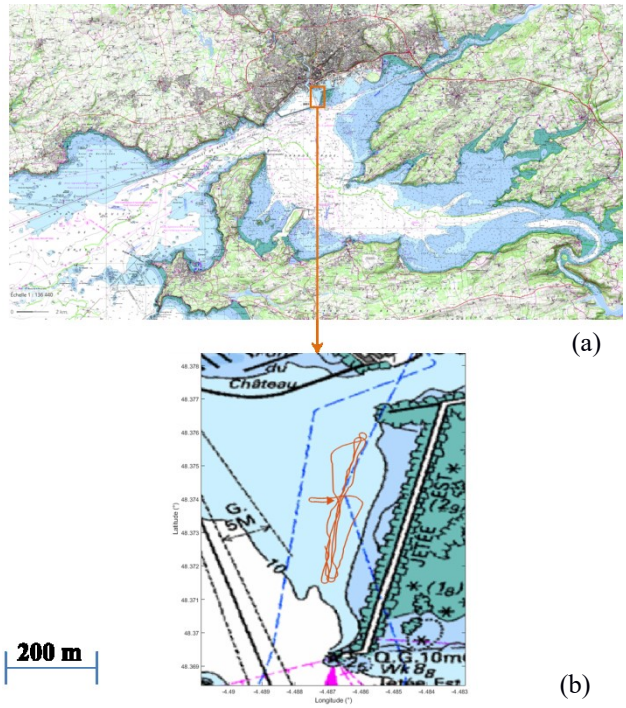
Figure 1. (a) Experimental protocol to track the SSS with a FLS. (b) Sonar position relative to the GNSS.

Nominal frequency	450 kHz
Range used in the survey	50 m
Pulse	Chirp of 400µs
Vertical beam	60° @-3dB
Horizontal beam	1.7° @-3dB
Emitted level	<210dB re 1µPa @1m

Table 1. Principal characteristics of the SSS Starfish 450 during the experiment [6]

Operating Frequency	900 kHz
Ping Rate	10 Hz
Field-of-View	130°
Range used in the survey	17 m
Beam Width	1° x 20°
Number of Beams	768
Beam Spacing	0.18°
Range Resolution	1 in

Table 2. Principal characteristics of the FLS BlueView P900-130 during the experiment [7]



(a) (b)

Figure 2. (a) Area of the experiment. (b) Trajectory realized during the experiment (in brown), overprinted on the bathymetric map.

3. TRACKING OF THE FISH REFLECTOR IN THE FLS IMAGE

3.1 Description of the algorithm

The first task which should be processed is the tracking of the target corresponding to the SSS in the FLS image. **Figure** 3 shows an example of the SSS signature in the FLS image. The different positions of the SSS in the FLS image will vary according to the time, so an iterative image processing module is realized to obtain the different positions of the SSS in the FLS image. This module is working as follow:

- For the first iteration, an approximate position of the target in the FLS image is given. This position is automatically refined by finding the maximal luminance in the neighboring of ± 5 pixels
- For the next iterations, positions are researched in the neighboring of the previous position in the FLS image.
    - To find possible targets corresponding to the SSS, a subimage is extracted from the FLS image around the previous position (± 5 pixels).
    - Then, areas corresponding to possible targets are extracted by thresholding: the threshold is automatically computed as $th = \overline{I_{sub}} - 5$, where $\overline{I_{sub}}$ is the average value of the sub-image.
    - Little areas (<10 pixels²) are removed.
    - Finally, position is given as the coordinate of the centroid of the area closest from the position of the previous iteration.

Figure 4 shows a schematic of the tracking process and **Table** 3 reminds the principal parameters of the tracking process in FLS images.

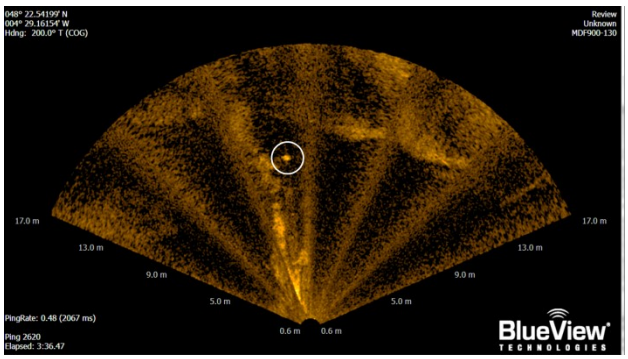


Figure 3. Example of image showing the SSS signature in the FLS data (surrounded by white)

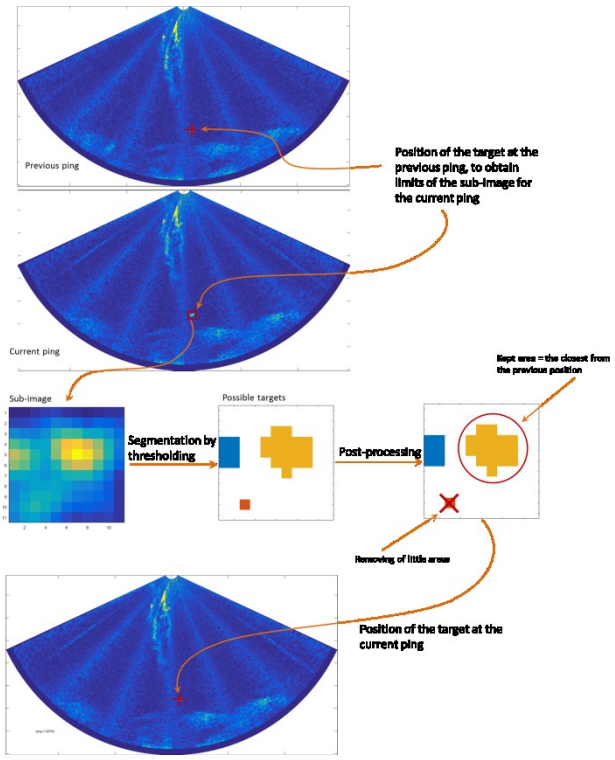


Figure 4. Schematic of the tracking process.

Size of the sub-image	5 x 5 pixels around the previous position of the target
Threshold used for the segmentation of the sub-image	as $th = \overline{I_{sub}} - 5$, where $\overline{I_{sub}}$ is the average value of the sub-image
Minimal size of the segmented areas	10 pixels²

Table 3. Principal parameters of the tracking process.

3.2 Tracking results analysis

An example of tracking result is presented in **Figure** 5. The cable length is quite the same during all the survey, so, the principal displacement is across-track, with a maximal amplitude of about 5 meters. The interest of using such a device to obtain the real position of the SSS is then obvious: indeed, with an absence of a tracking system, a simple layback should be added to obtain an estimation of the SSS position, which can produce an error of about 5 meters, at least across-track.

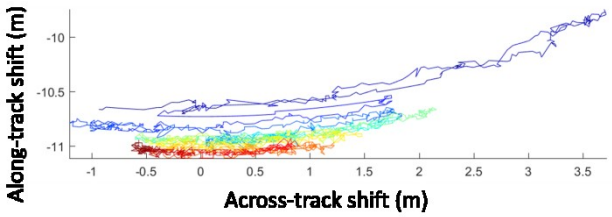


Figure 5. Tracked SSS positions in the FLS image. Positions are here presented in the FLS baseline (positive across-track values at starboard and negative along-track values behind the FLS). Colors are representing time passing (blue for the first pings to red for the last pings)

4. PROJECTION OF THE SONAR IMAGE IN A GIS: THE DIFFERENT STEPS

Once the tracking process of the SSS in FLS images is realized, SSS mosaic can be computed. The different steps are:

- Projection of SSS towfish positions in a GIS for each ping in UTM system
- Affectation of a geographical position for each point of SSS image
- Transformation of UTM coordinates to latitude/longitude coordinates (optional)
- Interpolation in a regular grid.

4.1 Projection of SSS towfish positions in a GIS

So, the first step is the projection of SSS towfish positions in a GIS, as explained in equations (1) and (2).

$$x_{trajsss_{geo}} = -\sin(ang)\, x_{trajsss} + \cos(ang)\, y_{sss} + x_{ship} \quad (1)$$

$$y_{trajsss_{geo}} = \cos(ang)\, x_{trajsss} + \sin(ang)\, y_{sss} + y_{ship} \quad (2)$$

With:

- $(x_{trajsss}, y_{trajsss})$ positions coordinates of the SSS in the boat reference system. If the FLS and the GNSS are located at the same point, coordinates are the same as explained at the previous paragraph (in meters), if it is not the case, a transformation should be made to take into account FLS position relative to the GNSS. In this experiment, the FLS was not at the same place than the GNSS but was insonifying in a direction parallel to the boat reference, so, a simple translation of (–1.145 m, 1.2565 m) is necessary to obtain coordinates.
- (x_{ship}, y_{ship}) geographical coordinates of the vessel (given by the RTK GNSS, in UTM system)
- and $ang = 90 - heading$, the heading being estimated from GNSS data (so, it is the heading of the ship and not strictly the heading of the towfish, but, in absence of measures of the towfish heading, these values will be considered as a good approximation of the heading for the towfish).

An example of the estimate towfish trajectory can be shown on **Figure** 6, which also shows the ship trajectory and an estimation of the range of the sonar for each ping.

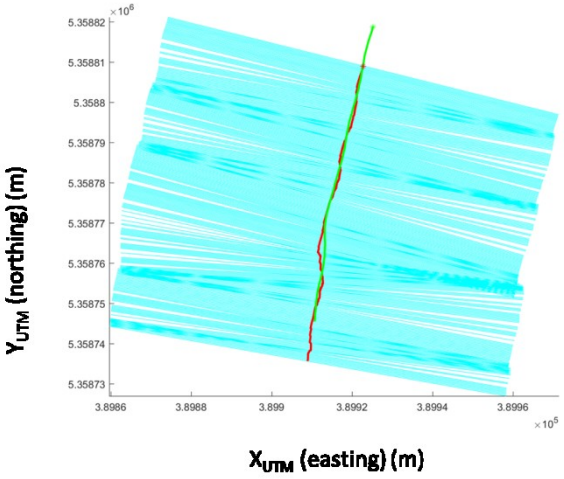


Figure 6. Example of SSS trajectory (in red) comparing to the ship trajectory (in green). Cyan lines represent SSS range at each ping (lines are not parallel due to the heading)

4.2 Coordinates of each point of a ping in towfish baseline

The next stage is the affectation of coordinates for each point of a ping in the towfish baseline. To do that, each point of a ping is associated with coordinates, referenced to the center of the towfish. A prior task is to remove the water column, so the across-track distance should be modified to take into account the effect of the projection of the acoustic beam on the seabed. The horizontal distance is then equation (3):

$$x_H = \sqrt{d^2 - h^2} \quad (3)$$

where *h* is the height of the water column and *d* the slant range (only valid for $d > h$).

The vector $x_{sss_{towfish}}$ takes the different values of x_H for the positive values and $-x_H$ for the negative values (equation (4)).

$$x_{sss_{towfish}} = [-x_H, x_H] \quad (4)$$

As for values of $y_{sss_{towfish}}$, they are null because the reference is the towfish (equation (5)):

$$y_{sss_{towfish}} = 0 \text{ for all pings} \quad (5)$$

4.3 Affectation of a geographical position for each point of SSS image

The next stage is the projection of each point of the SSS waterfall image in the GIS. Then, each point of the SSS image is projected in the GIS (equations (6) and (7)):

$$x_{imgsss_{geo}} = -\sin(ang)\, x_{sssTowfish} + x_{trajsss_{geo}} \quad (6)$$

$$y_{imgsss_{geo}} = \cos(ang)\, x_{sssTowfish} + y_{trajsss_{geo}} \quad (7)$$

4.4 Interpolation in a regular grid

At this stage, each point of the SSS waterfall image is associated to a geographical coordinate. The last step is the transformation of each coordinate from UTM to latitude, longitude values and a projection in a regular grid via an interpolation on a regular grid. Finally, mosaic image of SSS data is obtained. An example of SSS mosaic is shown on **Figure 7**.

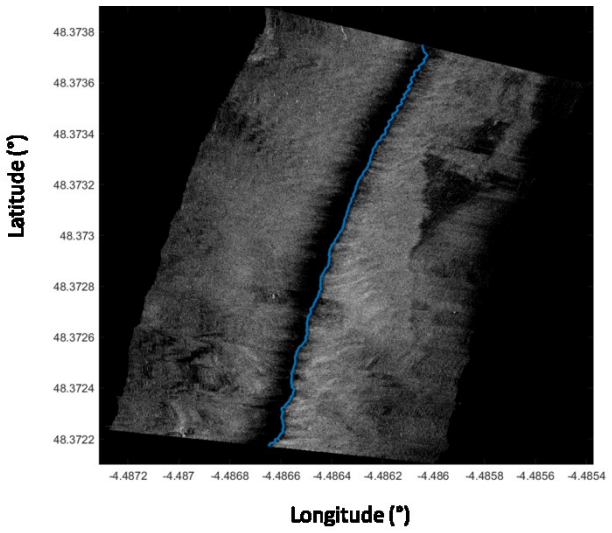


Figure 7. Example of SSS mosaic

5. COMPARISON WITH A DTM

5.1 DTM of the area

The DTM of the area can be used as the ground truth. In particular, positions of objects present on the SSS mosaic will be compared with positions of the same objects in the DTM. As it can be shown on the **Figure** 8, it is not easy to see little objects on the DTM, because of the large range of depths (~20 m) comparing to the height of the possible objects (<1 meter). So, to easily locate little objects, an image of local standard deviation of the bathymetry is generated, as shown on **Figure** 9.

Objects positions extracted from SSS mosaics should now be compared with objects positions extracted from the DTM. Each time, two cases will be tested:

- Use of the FLS tracking (work presented in the previous paragraphs)
- Use of a simple layback: instead of having the real position of the SSS relative to the vessel, a simple layback should be added to the ship position.

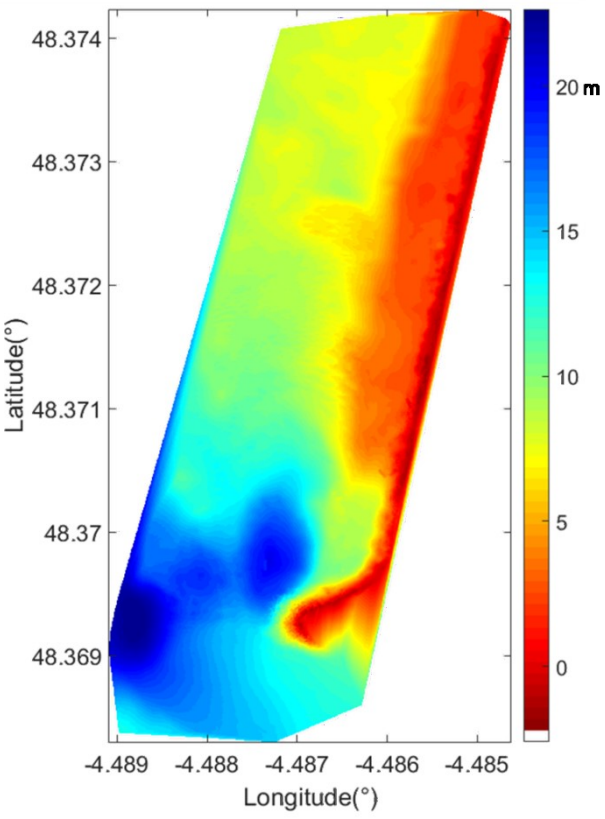


Figure 8. DTM of the area

5.2 Positions comparisons for SSS mosaics using the FLS position tracking

Several SSS images are used in this comparison, all approximately oriented north to south. For each mosaic, positions of several objects are extracted and compared to positions coming from the DTM. An example of positions of a same object coming from all mosaics is shown on **Figure** 10. In this example, positions are plotted on the DTM standard deviation map.

Distances between the different objects in the different mosaics and their corresponding objects in the DTM are presented on **Table** 4 (in meters). It shows of about one meter between SSS mosaics and the DTM, knowing that most of these objects have a size over one meter. So, positioning precision seems to be quite accurate.

However, position errors seem to be systematically more on the east, except for few contacts. On the other side, contacts are sometimes more on the north, sometimes more on the south. At this stage, it is not possible to give a correct explanation for this, especially the offset to east: in fact, objects was sometimes at portside, sometimes at starboard, sometimes near the SSS, sometimes farther and the surveys are sometimes from north to south or from south to north. Maybe the fact that the considered

heading is the boat heading and not the real SSS towfish heading can explain a part of this imprecision.

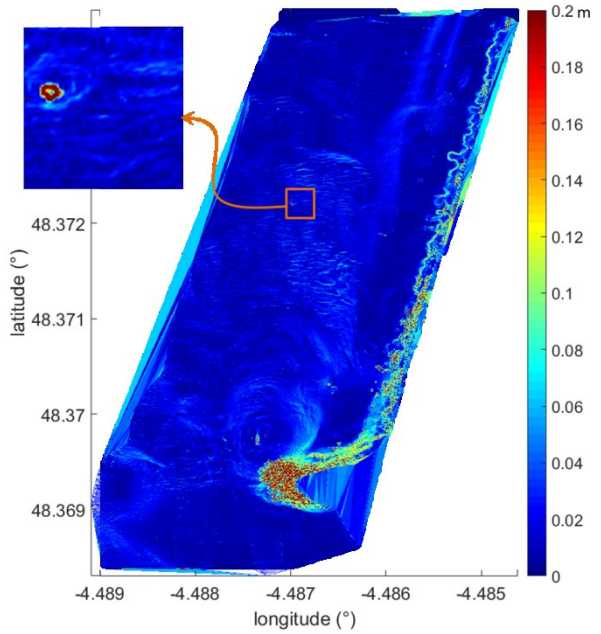


Figure 9. local standard deviation of the DTM: little objects can be easily detected.

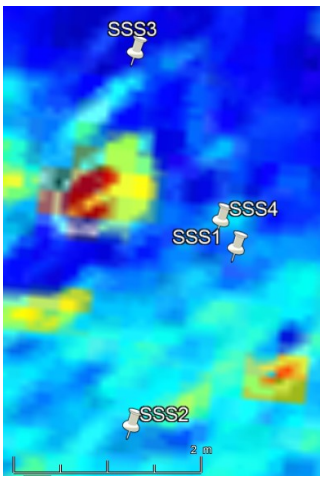


Figure 10. Positions of a same object in the different SSS mosaics, plotted on the DTM standard deviation map. The considered object is the red disk on the left.

5.3 Positions comparisons for SSS mosaics using the FLS position tracking *vs.* using a simple layback

Instead of using a FLS tracking to obtain the SSS position, a simple layback should be added to the ship position: in this case, the towfish is considered just behind the ship, with a distance function of the cable length. A comparison should be then realized between object positions obtained with a FLS tracking and with a layback of 10 m, which is corresponding to the cable length. The **Figure** 11 shows the positions of the same object in the SSS mosaics, plotted in the DTM. As for the previous case, distances between mosaics objects positions and DTM objects positions are estimated (**Table** 5).

	Mosaic number	Δx (m)	Δy (m)	Δd (m)
Elongated object	SSS2	2.57	-1.05	2.78
	SSS3	-0.95	0.57	1.11
Anchor block	SSS3	-0.12	1.67	1.67
	SSS4	-0.12	1.23	1.23
Pockmark	SSS3	0.38	0.55	0.67
Double pockmark	SSS1	1.69	-0.48	1.76
	SSS2	0.54	-2.79	2.84
	SSS3	0.26	1.89	1.9
	SSS4	1.48	-0.14	1.49

Table 4. Positions differences between the different objects and the different SSS mosaics obtained with FLS tracking and DTM (from UTM coordinates, in meters).

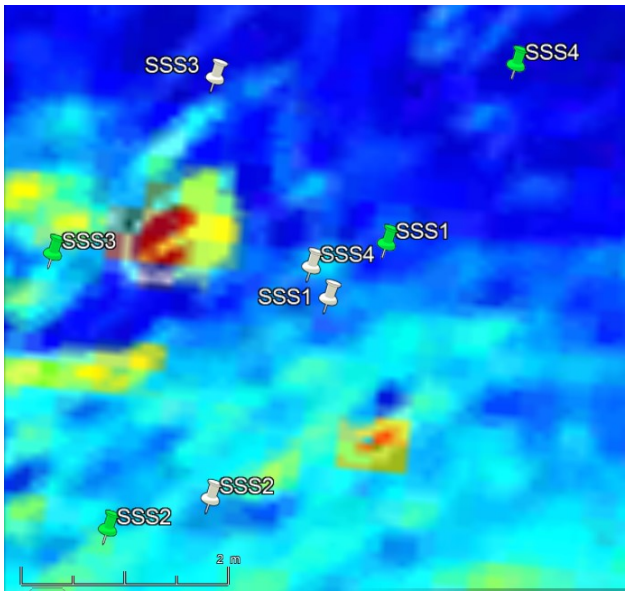


Figure 11. Positions of a same object in the SSS mosaics, plotted on the DTM standard deviation map. The considered object is the red circle on the left. White marks, use of FLS tracking, green marks, use of a layback of 10 m.

As it can be seen, most of objects positions obtained with FLS tracking are closer to the DTM than the same objects positions obtained with a simple layback. For the layback, positions seem to be rather randomly distributed, due to the fact that the SSS was sometimes more on the left of the boat, or sometimes more on the right, but considered just behind. The average and standard deviation distances to the objects, all over the contacts are

shown on **Table** 6. As it can be seen, results are better for the FLS tracking than the layback.

However, these statistics are realized only on few contacts and few mosaics. To see the advantage of using the FLS tracking, it should be interesting to obtain an estimation of position difference using a high number of objects. Unfortunately, it is not possible in this experiment. Another surveys should be realized to obtain statistics of position differences.

	Mosaic number	Δx (m)	Δy (m)	Δd (m)
Elongated object	SSS2	0.14	-0.56	0.58
	SSS3	-3.14	-1.38	3.43
Anchor block	SSS3	-2.31	-0.51	2.36
	SSS4	3.47	3.27	4.77
Pockmark	SSS3	-2.24	-0.73	2.35
Double pockmark	SSS1	2.3	0.18	2.31
	SSS2	-0.58	-3.21	3.27
	SSS3	-1.41	-0.2	1.42
	SSS4	3.6	2.27	4.25

Table 5. Positions differences between the different objects and the different SSS mosaics obtained with a layback of 10 m and DTM (from UTM coordinates, in meters).

	FLS tracking	Layback
Average distance from DTM (m)	1.71	2.74
Standard deviation distance from DTM (m)	0.72	1.32

Table 6. Average and standard deviation positions differences between the different objects and the different SSS mosaics obtained with the FLS tracking or a layback of 10 m and DTM (from UTM coordinates, in meters).

6. CONCLUSION AND PERSPECTIVES

The principal objective of the work presented here was to estimate the feasibility of using a FLS to track towfish positions during a survey. Usually, to take into account the towfish position, a simple layback is added but it can generate positioning errors, due to a drift of the towfish or a cable not sufficiently tensioned. A more sophisticated process consists in using a USBL system to have the real position of the SSS with respect to the ship. Unfortunately, this device is not always available or suitable (case of a magnetometer for example, where measures can be perturbed by the acoustic transponder). So, a solution should be the use of a FLS to track towfish positions.

The application proposed here was intentionally SSS mosaic, because of the possible comparison with a DTM. So, the rest of the work was consisting in realizing a georeferenced SSS image mosaic, considering in particular the real position of the SSS towfish with respect to the ship.

In a first part, the description of the experiment was realized, especially to show how the FLS was placed to track the SSS. The navigation data was also shown on a bathymetric map of the area.

A second part was devoted to a description of the tracking algorithm. Actually, this algorithm is quite simple, and consisting in a target detection by segmenting FLS image with a threshold in the neighborhood of the SSS localization at the previous ping.

The third part is the projection of SSS positions in a GIS. This projection uses SSS localizations in the FLS baseline previously estimated and ship positioning, provided by a RTK GNSS. At this stage, SSS mosaics are obtained and can be projected in a GIS.

The last part of this work is a comparison of objects localization both on SSS mosaics and on DTM. Actually, four surveys of the same area are compared, with only few objects available, showing a distance of less than one meter between SSS positions and DTM positions. Finally, it shows that using FLS tracking seems to give best results than using a simple layback, even if this last affirmation should be confirmed by other objects positions.

Several improvements can be proposed. Firstly, the tracking algorithm is very simple and should be made more reliable. The help of algorithms such optical flows should help to obtain it. Also, the use of Kalman filters should be a good choice to improve tracking results.

A second amelioration should be to have a precise estimation of the SSS heading. Indeed, actually, in the absence of the real values of SSS towfish heading, the ship heading is used. But there is no evaluation of the error made. So, it should be necessary to obtain an estimate of this mistake, or, better, a forecast of the real SSS towfish heading.

To obtain precise values of the georeferencing accuracy, an effort should also be made to compare SSS mosaics results to the ground truth. Two ways can be used. The first one is to compare positions of many objects both in SSS mosaics and in DTM as made in this work for the four objects. Having a sufficiently number of objects should allow to obtain statistical values of the accuracy of the process. A second way should to have in a same survey a FLS tracking and an USBL positioning. Indeed, the accuracy of such a system is known, and would be compared to the proposed process.

Finally, this system should be extended to another towfish, for example magnetometers, to obtain precise map of magnetic anomalies, or ROV, for example to obtain georeferenced photography.

7. ACRONYMS

DTM: Digital Terrain Models

FLS: Forward Looking Sonar

GIS: Geographical Information System

GNSS: Global Navigation Satellite Systems

LBL: Long Baseline

ROV: Remotely Operated Vehicle

RTK: GNSS: Real Time Kinematic GNSS

SSS: Sidescan Sonar

USBL: Ultra-Short Baseline

UTC: Coordinated Universal Time

UTM: Universal Transverse Mercator

8. ACKNOWLEDGMENTS

Authors want to thank all coworkers who help them during the experiment, especially Pierre Simon, Romain Schwab from ENSTA Bretagne and Isabelle Delumeau from Ecole Navale. Authors also thank Nathalie Debese from ENSTA Bretagne to provide the DTM of the area.

9. REFERENCES

[1] X. Lurton: *An Introduction to Underwater Acoustics. Principles and Applications*, Springer-Verlag Berlin Heidelberg, 2010.

[2] K. Camidge et *al*: *Developing Magnetometer Techniques to Identify Submerged Archaeological Sites*: Theoretical Study Report, Historic Environment Council, Cornwall Council, 2010.

[3] A. M. Crawford: *Methods of Determining Towfish Location for Improvement of Sidescan Sonar Image Positioning*: Technical Memorandum DRDC Atlantic TM 2002-019, 2002

[4] P. Blondel: *The Handbook of Sidescan Sonar. Springer*, Praxis. Chichester 52-55, 2009

[5] M. Gendron: "Algorithms and Data Structures for Automated Change Detection and Classification of Sidescan Sonar Imagery", *University of New Orleans Theses and Dissertations,* 2004.

[6] Tritech. *Product Datasheet of the Starfish 450 F sidescan sonar*. https://www.tritech.co.uk/media/products/side-scan-sonar-shallow-water-starfish-seabed-imaging-systems.pdf?id=95d06fa8

[7] BlueView. P900 Series 2D Imaging Sonar Datasheet. https://rts.as/wp-content/uploads/2018/09/Teledyne-Blueview-P900-Series-Sonar.pdf

[8] P. Cervenka, C. de Moustier and P. F. Lonsdale: "Geometric Corrections on Sidescan Sonar Images based on Bathymetry. Application with SeaMARC II and Sea Beam Data.", *Marine Geophysical Researches* 16: 365-383, 1994.